Heliyon 9 (2023) e16137

Contents lists available at ScienceDirect

Heliyon

journal homepage: www.cell.com/heliyon

Research article

Green-synthesized nanoparticles of the polyherbal extract attenuate the necrosis of pancreatic β-cell in a streptozotocin-induced diabetic model

Muhammad Abid Hasan Chowdhury [a], Salahuddin Quader Al Araby [a], Walla Alelwani [b], Shahad W. Kattan [c], Omniah A. Mansouri [d], Mohammad Rasib Uddin Rahat [e], Mala Khan [f], Jitbanjong Tangpong [g], Md. Atiar Rahman [a,g,*]

[a] *Department of Biochemistry & Molecular Biology, University of Chittagong, Chittagong-4331, Bangladesh*
[b] *Department of Biochemistry, College of Science, University of Jeddah, Jeddah, Saudi Arabia*
[c] *Medical Laboratory Department, College of Applied Medical Sciences, Taibah University, Yanbu, Saudi Arabia*
[d] *Department of Biology, Collage of Science, University of Jeddah, Saudi Arabia*
[e] *Department of Pharmacy, International Islamic University Chittagong, Kumira, Sitakunda, Chittagong-4318, Bangladesh*
[f] *Bangladesh Reference Institute for Chemical Measurements (BRiCM), Dr. Qudrat-i-Khuda Road, Dhanmondi, Dhaka-1205, Bangladesh*
[g] *School of Allied Health Sciences, Walailak University, Nakkhon-Shi Thammarat, Nakhon Si Thammarat, 80160, Thailand*

ARTICLE INFO

Keywords:
Antihyperglycemic polyherbal
Antioxidant
Green-synthesized nanoparticle

ABSTRACT

Plant-based nanoformulation is one of the novel approaches for therapeutic benefits. This research synthesized a silver nanoparticle from the polyherbal combination of four plants/seeds (*Momordica charantia*, *Trigonella foenum*-graecum, *Nigella sativa*, and *Ocimum sanctum*) and investigated its antidiabetic effects in streptozotocin-induced Wistar albino rat model. The polyherbal extract (PH) was extracted by the Soxhlet-solvent extraction method and the resulting crude extract was undergone for silver nanoparticle synthesis. The PH extract was subjected to a four-week intervention in fructose-fed streptozotocin-induced Wistar Albino rats' models and in vitro antioxidative tests. Experimental animals (age: 6–7 weeks, male, body weight: 200–220 g), were divided into five groups including normal control (NC), reference control (RC), diabetic control (DC), and treatment groups PH200, PH100, and PHAgNP20. After three weeks of intervention, body weight, weekly blood glucose level, oral glucose tolerance test, AST, ALT, alkaline phosphatase, total cholesterol, triglycerides, uric acid, urea, and creatinine level of PH200 were found to be significantly ($P < 0.05$) improved compared to the diabetic control. The same dose demonstrated better regeneration of damaged pancreatic and kidney tissues. In vitro antioxidant assay manifested promising IC50 values of 86.17 μg/mL for DPPH, 711.04 μg/mL for superoxide free radical, and 0.48 mg/mL for Iron chelating activity of the polyherbal extract. GC-MS analysis impacted the major volatile compounds of the PH. The data demonstrate that the PH and its nanoparticles could be a novel source of antidiabetic therapeutics through an advanced dose-response study in the type 2 diabetic model.

* Corresponding author. Department of Biochemistry and Molecular Biology, University of Chittagong, Chittagong-4331, Bangladesh and School of Allied Health Sciences, Walailak University, Thailand.
E-mail address: atiar@cu.ac.bd (Md.A. Rahman).

https://doi.org/10.1016/j.heliyon.2023.e16137
Received 23 October 2022; Received in revised form 21 April 2023; Accepted 6 May 2023
Available online 15 May 2023
2405-8440/

1. Introduction

Diabetes mellitus is an endocrine metabolic disease defined by hyperglycemia brought on by insufficient amounts of either insulin or the insulin receptor [1]. Currently, 537 million people suffer from diabetes mellitus, and this is one in ten people. This number is estimated to reach 643 million by 2030 and 783 million by 2045 [2]. Diabetes is a silent killer that can cause a variety of pathologies, including cardiomyopathy, nephropathy, retinopathy, neuropathy, coronary artery disease, and stroke [3,4]. Glycemic control has

Abbreviations

PH	Polyherbal extract
AgNP	Silver nanoparticle
DPPH	1,1-diphenyl 2-picryl hydrazyl
TPC	Total phenolic content
TFC	Total flavonoid content
DM	Diabetes mellitus
STZ	Sterptozotocin
ALT	Alanine aminotransferase
AST	Aspertate aminotransferase
ALP	Alkaline phosphatase
DMSO	Dimethyl sulfoxide

been recognized as the primary therapeutic intervention in diabetes mellitus, even though many risk factors in diabetes and deadly consequences need the development of novel treatment techniques for efficient diabetes management [3]. However, the commercially available anti-diabetic drugs disappoint physicians and patients due to their side effects, shifting the attention to discovering innovative antidiabetic medications. Plant-based therapeutics are usually thought to be less or nontoxic and free of adverse effects [5]. So, considering the cost and adverse effects of synthetic drugs, novel, and effective alternative antidiabetic sources are under strong surveillance [6]. Additionally, a drug's bioavailability is constrained by a complex drug molecule, which reduces drug absorption. Plant-based nanoparticles have unprecedented attention for drug formulation especially drug delivery by utilizing their small size and large surface area which facilitated cross the blood-brain barrier, entry into the pulmonary system, and to be absorbed through the endothelial cell of the skin leading to an increase in the bioavailability of the drug [7]. This justifies the use of plant extract-based nanoparticles as one of the best options to improve the drug's bioavailability [8]. Silver nanoparticles enable the extensive use of natural resources such as plants, fungi, bacteria, and actinomycetes more safely and cost-effectively by avoiding the use of hazardous chemicals, high temperatures, and pressures. They are also affordable to use in biomolecular detection, catalysis, drug delivery in pharmaceuticals, and biosensors in diagnosis [9]. Its extensive medicinal activities as antidiabetic, anti-inflammatory, anti-bacterial, and anti-viral are thought to be because of its physiochemical properties [10,11]; gained by green synthesis processes of biological application [12].

Of the four approached plant materials, *Momordica charantia* is a Cucurbitaceae family plant distributed in tropical and subtropical Africa, Asia, and Australia. It is the most popular among cylindrical shape vegetables, used to produce floral oil and in Chinese folk medicine. *Momordica charantia* is known to many people for its anti-diabetic action [13]. *Nigella sativa* is known as "Holly Seed", native to Asia mainly in the southern and western parts of Asia, Southern Europe, and the Middle East. Although it is known for the treatment of all diseases, its antidiabetic effect has been scientifically reported quite a bit late [14–16]. *Trigonella foenum-graecum*, commonly known as "Fenugreek" is widely used as a spice, vegetable, and beautifying agent, and it has great nutritional and medicinal value while its traditional use in lowering blood glucose and cholesterol level is also well-cited [17,18]. The plant, *Ocimum sanctum,* is native to South Asia, Southwest Asia, and the Northern part of Australia. It is a common traditional therapeutic agent, for headaches, stomach disorders, and diabetes [19,20]. Due to their antidiabetic potentials, this research hypothesized to formulate of a polyherbal extract with the combination of these four plants/seeds to investigate their antidiabetic effects as green-synthesized Ag-nanoparticles especially focusing on how the nanoparticles of polyherbal extract improve the pancreatic dysfunction in streptozotocin-induced diabetic models.

2. Materials and methods

2.1. Chemical and reagents

The 2,2-Diphenyl-1-picrylhydrazyl (DPPH), nitro blue tetrazolium (NBT), Streptozotocin, dimethyl-sulfoxide (DMSO $\geq$99.5%), Gallic acid (ACS reagent, $\geq$98.0%), Curcumin (Purity$\geq$ 80%), L-Ascorbic acid (Purity 99%), Potassium Phosphate monobasic (Purity $\geq$99%), Potassium phosphate dibasic (Purity $\geq$98%), Folin-Ciocalteu reagent, Silver nitrate (analytical grade), *O*-phenanthroline and ethanol (99%) purchased from Sigma-Aldrich, Co. (St. Louis, USA), were used for this experiment. All chemicals and reagents were of the analytical grade until described otherwise.

2.2. Collection and identification of the samples

The four plants/seeds *(*detailed in Table 1*)* were collected from the local market of Chittagong City, Bangladesh. Although they are very commonly known, their scientific and taxonomic identification as *Momordica charantia, Trigonella foenum-graecum, Nigella sativa, and Ocimum* sanctum was assisted by Dr. Shaikh Bokhtear Uddin, Taxonomist, and Professor, Department of Botany, University of Chittagong. They are preserved in our institutional herbarium with the accession numbers of *Momordica charantia*-CUBH-19*, Trigonella foenum-graecum*- CUBH-20*, Nigella sativa- CUBH-21, and Ocimum* sanctum- *CUBH-22.*

2.3. Preparation of the polyherbal extract (PH)

After collection, all the samples were washed with tap water to remove sand or other debris. Green *Momordica charantia* fruits were chopped into small pieces. Pieces of *M. charantia*, *T. foenum-graecum seeds, N. sativa seeds,* and *O. sanctum* leaves were dried in an incubator at 50 °C. Dried samples were then ground to powder separately and homogeneously mixed in a ratio of 5:2:2:1 (MC:TF:NS: OS) based on their cited polyphenolic contents. One hundred grams of mixture required 50 g of *M. charantia*, 20 g of *T. foenum-graecum seeds,* 20 g of *N. sativa seeds,* and 10 g of *O. sanctum* The resulting mixture was moved to prepare crude extract with distilled water using Soxhlet apparatus at boiling temperature (80°-100 °C) until decolorization of the mixture. A dark color liquid extract was formed which was filtered through a Whatman No. 1 filter paper. The filtrates were collected in a conical flask. These clear filtrates were evaporated to dry forming a sticky semi-solid crude extract by rotary evaporator *(*RE 200, Bibby Sterling Ltd, UK*)*. Eight (8.0 g) of polyherbal crude extract was obtained from 100 g of dried mixed polyherbal powder. The polyherbal extract (PH) was preserved in the refrigerator at 4 °C for further analysis.

2.4. Preparation of silver nitrate ($AgNO_3$) nanoparticles of polyherbal extract

Five mL of liquid extract *(*con^n 5 mg/mL*)* was added dropwise to a conical flask containing 95 mL of 1 mM silver nitrate solution and stirred vigorously with a magnetic stirrer for 8 h at 37 °C. The solution was then centrifuged at 5000 rpm for 20 min. The supernatant was discarded, and the final residue was washed with sterile distilled water and dried. This sample was preserved at 4 °C for further characterization and *in vivo* analysis.

2.5. Phytochemical screening

2.5.1. Qualitative phytochemical screening

The phytochemical screening for carbohydrates, proteins, steroids, tannins, saponins, and cardiac glycosides was conducted by using the established test methods [21]. In each test, a 10% (w/v) solution of the polyherbal extract was taken and tested.

2.5.2. Determination of total flavonoid content (TFC) and total phenolic content (TPC)

The total flavonoid content in PH was determined by the aluminium chloride colorimetric method [22]. Briefly, 1 mL of PH or gallic acid (standard) of different concentrations was taken in screw cap test tubes. Then 3 mL of methanol, 200 μL of 10% aluminium chloride, 200 μL of 1 M potassium acetate, and 5.6 mL of distilled water were added to the test tubes respectively. Tubes were incubated for 30 min and read at 420 nm using a spectrophotometer (UV-VIS 1280, Shimadzu Corporation, Japan).

The content of total phenol (TPC) in PH was determined by the Folin-Ciocalteau reagent method [23]. A 0.5 mL of PH or gallic acid of different concentrations (800-50 μg/mL) was taken in a test tube. Then 2.5 mL of 10 times diluted Folin-Ciocalteau reagent solution was added. The resulting solution was added with 2.5 mL of 7.5% sodium carbonate. All the test tubes were then incubated for 20 min at 25 °C and absorbance was taken at 760 nm.

2.5.3. Assay of DPPH free radical scavenging activity

The DPPH free radical scavenging ability of PH was determined by the method described by Sanja et al. [24]. The PH was dissolved in methanol-water (50:50) to make a stock solution for serial dilution to 800- 50 μg/mL. Two mL of PH solution of different concentrations was taken, and 3 mL of DPPH solution (0.004%) was added. The test tube was incubated for 30 min at room temperature to

Table 1
Characterization of plant materials.

Sample Name	Plant Part	Collection area	(GPS location)	Accession Number	Physical status
Momordica charantia L.	Whole fruit (excluding seed)	Karnafuli Market, Chittagong	22.367063, 91.820444	CUBH-19	Green
Trigonella foenum-graecum L.	Seed	Karnafuli Market, Chittagong	22.367063, 91.820444	CUBH-20	Golden to Yellow color seed
Nigella sativa L.	Seed	Karnafuli Market, Chittagong	22.367063, 91.820444	*CUBH-21*	Black dried seed
Ocimum sanctum Linn.	Leaf	Pitambar Shaha Store, Khatunganj Road, Chittagong	22.339303, 91.842380	*CUBH-22*	Dry leaf

read at 517 nm.

The percentage of DPPH scavenging activity was calculated by the following equation:

$$\text{Percentage of scavenging activity} = \frac{Control - Test\ absobance}{Control} \times 100$$

2.5.4. Assay of superoxide scavenging activity

The superoxide scavenging activity of the extract of PH was determined by the alkaline DMSO method described by Ref. [25]. Briefly, PH was dissolved in alkaline DMSO (1.0mLDMSO containing, 5 mM NaOH in 0.1 mL water) to make a stock solution of 800 μg/mL to be diluted at 400-50 μg/mL concentration of PH. Blank was prepared by using 0.1 mL NBT solution in 1.0 mL DMSO solution. 0.1 mL NBT (1.0 mg/mL solution in DMSO) solution was taken in a test tube and 2 mL of the polyherbal extract was added to the test tube followed by the addition of 1 mL of alkaline DMSO. Curcumin was used as standard, and the absorbance was taken at 560 nm to calculate the scavenging effect:

$$\text{Percentage of scavenging activity} = \frac{Test\ absobance - Control}{Test\ absorbance} \times 100$$

2.5.5. Iron chelating effect activity of polyherbal extract

The iron chelating effect of PH was determined by Benzie and Strain's method [26]. A 2 mL of the PH (1 mg/mL) was dissolved with distilled water to prepare the solution of different concentrations of 0.5–0.0625 mg/mL. Then 1 mL of 1,10-phenanthroline (0.05%) and 2 mL freshly prepared ferric chloride (200 μg/mL) were added, and the absorbance was taken at 510 nm. Ascorbic acid was used as the standard to calculate the iron chelating activity of PH:

$$\text{Percentage of scavenging activity} = \frac{Test\ absobance - Control}{Test\ absorbance} \times 100$$

2.5.6. GC-MS analysis

The volatile compounds extracted from the were analyzed by gas chromatography (GC-2010 plus, Shimadzu Corporation, Kyoto, Japan), coupled with a mass spectrometer (GCMS- TQ 8040, Shimadzu Corporation, Kyoto, Japan). A fused silica capillary column (Rxi-5ms; 30 m, 0.25 mm ID, and 0.25 μM) was used for GC maintaining sample inlet temperature at 250 °C. A1μL sample was injected in splitless mode. The oven temperature was programmed as 75 °C (1 min); 25 °C, 125 °C (1 min); 10 °C, and 300 °C (15 min). The aux (GC to MS interface) temperature was set to 250 °C. The total run time was 36.50 min, and the column flow rate was 1.5 mL/min He gas. An electron ionization (EI) type mass spectroscopy (MS) was used in Q3 scan mode. 200 °C ion source temperature, 250 °C interface temperature, 1.17 kV detector voltage, and 50–1000 *m/z* mass range were set for MS. Individual compounds with *m/z* ratio were searched in "NIST-MS Library 2014. Total Ionic Chromatogram (TIC) was used to determine the peak area as well as the percentage amounts of each compound.

2.5.7. Green synthesis of silver (Ag) nanoparticles

Silver nanoparticles were synthesized by a slight modification of the method of Suresh et al. and Govindaraju et al. [27,28]. In a magnetic stirrer, 10 mL of the stored PH was blended with 50 mL 0.5 M $Ag(NO_3)\cdot 6H_2O$ solution and agitated at 60 °C for 30 min. A dropwise addition of 1 M NaOH solution was then made until a noticeable white precipitate appeared and, the reaction was allowed to run for 2 h at 80 °C. Following centrifugation of 20 min at 5500×*g*, the precipitates were washed several times with deionized water and stored at −80 °C. The precipitates were freeze-dried into powder using a LABCONCO 2.5 L refurbished freeze dryer/lyophilizer at −84 °C with 0.133 mBar vacuum pressure as part of the optimized conditions to achieve precise Ag nanoparticles.

2.5.8. Characterization of Ag-nanoparticles

To characterize the biogenic Ag-NPs, a UV–visible spectrophotometer (Shimadzu UV-160 A; range 190–1100 $cm^{-1)}$ was employed. The sophisticated analytical instrument facility at Bangladesh Atomic Energy Commission carried out the X-ray Diffraction (XRD), Scan Electron Microscopy with Energy Dispersive X-ray (SEM-EDX), and Fourier transforms infrared (FT-IR) spectroscopy (range: 400–4000 cm^{-1}) analysis for biochemical properties.

2.6. Experimental animals and their grouping

Thirty adult Wistar Albino rats *(*Age:6–7 weeks, Sex: Male, Body weight: 200–220 g*)* were randomly categorized into normal control *(*NC*)* administrated with distilled water, STZ-induced diabetic control *(*DC*)* administrated with distilled water, reference control *(*RC*)* administrated with metformin 250 mg/kg BW *(*MET250*)*, STZ-induced diabetic rat treated with the polyherbal extract 200 mg/kg BW *(*PH200*)*, STZ induced diabetic rat treated with the polyherbal extract 200 mg/kg BW *(*PH200*)*, STZ induced diabetic rat treated with the polyherbal extract 100 mg/kg BW *(*PH100*)* and STZ induced diabetic rat treated with the silver nanoparticle of the polyherbal extract 20 mg/kg BW *(*PHAgNP20*)*. Before starting the intervention, the animals were acclimatized under standard laboratory conditions (polypropylene cage diameter 25 × 16 × 13 cm^3, relative humidity 55.00 ± 5.0%, room temperature 23.0 ± 0.5 °C and 12 h light: dark cycle) for one week and were fed with commercial rat pellet diet *ad libitum* and distilled water throughout the experimental period. Experimental animals were handled by following the Institutional Ethical Guidelines of the Faculty of Biological

Sciences, University of Chittagong.

2.6.1. Diabetes induction and intervention

After one week of administration of fructose solution (10%), the animals fasted for 12 h before injecting Streptozotocin [29]. Then a single dose of streptozotocin (50 mg/kg BW), dissolved in citrate buffer (0.1 M, pH 4.5), was injected intraperitoneally into the animals of DC, RC, and PH200, PH100, and PHAgNP20 groups while only citrate buffer was injected to the NC group. After one week of STZ injection, the animal's blood glucose levels were checked by tail prick method and the animals with blood glucose levels >300 mg/dL (tail-prick method, Gluco Dr. Auto, China) were considered diabetic.

2.6.2. Oral glucose tolerance test

At the end of the third week of intervention, an oral glucose tolerance test was done. For performing this test, a single dose of D-glucose (2 g/kg BW) was given orally to each group of animals, and measured the blood glucose level at several time intervals (30, 60.90, and 120 min) after the dose of glucose.

2.6.3. Collection of blood and organs/tissues and analyses of serum

After 3 weeks of the intervention period, animals were sacrificed by using halothane anesthesia, and blood and organs including the pancreas and kidney tissues were collected. The whole blood samples were centrifuged at 3000 rpm for 15 min at 25 °C temperature to collect the serum preserved at −30 °C for further biochemical analysis. The collected organ from each animal was washed with 0.9% NaCl (normal saline) and wiped with tissue paper and weighed. The weighed organs were preserved with 10% buffered formalin for histological analysis. The serum was undergone for the analyses of alanine aminotransferase (ALT), aspartate aminotransferase (AST), serum alkaline phosphatase, serum total protein, total cholesterol, triglycerides, serum creatinine, serum urea, and serum uric acid levels.

2.6.4. Histopathological analysis

The histopathological samples were prepared and analyzed following the protocols adopted by Araby et al. [30]:

Tissue fixation and dehydration: The tissues were fixed in neutral buffered formalin solutions for 48 h to preserve tissue from degradation, and to maintain the structure of the cell and of sub-cellular components such as cell organelles. The vertical sections of tissues were taken by sharp blade for further processes. After fixation, the tissues were dehydrated by passing through ascending grades of ethanol (70%, 8o%, 90%, 100% vol/vol) for 1 h in each solution. The tissues were then passed through 100% ethanol three times to remove the water from the tissue.

Clearing, paraffin impregnation, and block preparation: Dehydration was followed by passing the tissues through a hydrophobic clearing agent xylene three times consecutively to remove the alcohol from the tissues which were then embedded in molten paraffin wax, the infiltration agent. The tissues were kept in the paraffin for 2 h to remove water from tissues and replaced in a medium to be solidified for sectioning. The paraffin along with tissues in the molds was allowed to cool and hardened. The hardened blocks containing the tissue samples were then ready for further procedures and preserved at 4 °C until the cross-section was done.

Slide preparation and staining: Paraffin-embedded sections were cut into 3–5 μm thick sections, using a semi-automated rotary microtome machine (Biobase Bk-2258, Laboratory Manual Microtome, China). The ribbons were mounted on a glass microscope slide avoiding the formation of any folding. The slides were then kept on a stretcher machine for 10 min and placed in an incubator at 60–70 °C for 30 min. The tissue slices were deparaffinized with xylene and rehydrated with various ethanol dilutions (100%, 90%, and 70%). Hematoxylin and eosin (H&E) were used to stain the sections.

Mounting and microscopic examination: The stained slides were mounted with DPX and covered with coverslips. Different parameters of pancreatic and kidney cellular conditions were observed under Olympus BX51 Microscope (10*X* and 40*X*) and the histopathological images were taken with the help of the Olympus DP20 (5 MP) system.

Table 2
Phytochemical Screening of polyherbal extract.

Name of Test		Observation	Findings
Test for Carbohydrate	Molisch Test	Violate color	Present
	Fehling Test	Brick red precipitate	Present
	Benedict Test	Green color	Present
Test for protein or amino acid	Biuret test	No violate or pink color	Absent
	Xanthoproteic Test	No purple or blue color	Absent
	Ninhydrin Test	No orange color	Absent
Test for Cardioglycosidase	Killer killiani Test	No bluish-green color	Absent
Test for Tanin and Phenol		White precipitates	Present
Test for Saponin	Foam Test	0.5 cm foam	Present
Test for Steroid	Wagner's Test	Reddish brown color	Present
	Salwaski's Test	Cherry red color	Present

3. Result

3.1. Qualitative phytochemical screening test, GC-MS analysis, and nano-characterization

The phytochemical screening test revealed the presence or absence of carbohydrates, proteins, flavonoids, tannins, phenols, saponins, steroids, and glycosides in the polyherbal extract (PH) (Table 2). The volatile compounds of GC-MS analysis are summarized in Table 3 and Fig. 1. The crystalline size of the nanoparticles has been analyzed using the peak profile broadening method using a high score Plus platform with the wavelength: k-alpha 1: 1.540598 [A], k-alpha 2: 1.544426 [A], K-alpha: 1.541874 [A]. A nanocrystal of Ag had given a cubic size of 12.9 [nm] (Fig. S1).

3.2. Antioxidative effect of PH

The PH was found to show a very promising antioxidative effect. The total phenolic and the total flavonoid contents of PH were found to be 207.50 and 630 mg/g dry weight, respectively. The inhibition concentrations (IC_{50}) in different antioxidative models were less than the cut-off value of <1000 μg/mL. The DPPH radical scavenging effect of PH and standard ascorbic acid were found to be 86.17 μg/mL and 5.63 μg/mL, respectively. The graphical presentation of the DPPH scavenging activity of PH and the standard is shown in Fig. 2a and b. The superoxide scavenging activity of PH and standard (curcumin) was found to be 711.04 μg/mL and 0.61 μg/mL, respectively (Fig. 2c and d). The IC_{50} values of PH and the standard (ascorbic acid) for iron chelating activity were found to be 0.48

Table 3
GC-MS Analysis of PH extract.

No.	Compound Name	Retention Time	Peak Area%
1	1,4,5,8-Tetraazadecalin	3.658	7.19
2	Benzeneacetaldehyde	3.708	4.10
3	2,5-Dimethylfuran-3,4(2H,5H)-dione	3.767	3.75
4	Methane, (methylsulfinyl) (methylthio)-	3.833	3.36
5	4-Methylpentyl pentanoate	3.892	3.75
6	Glycerin	3.975	13.92
7	2(5H)-Furanone, 3-hydroxy-4,5-dimethyl-	4.233	0.58
8	4H-Pyran-4-one, 2,3-dihydro-3,5-dihydroxy-6-methyl	4.725	3.14
9	2-Furanone, 3,4-dihydroxytetrahydro	4.9	1.30
10	5-Methoxypyrrolidin-2-one	5.025	1.11
11	Dodecane	5.217	2.40
12	3,4-Dihydroxy-5-methyl-dihydrofuran-2-one	5.4	0.80
13	Benzofuran, 2,3-dihydro-	5.467	0.96
14	Cyclooctanol, o-[5-[1-cycloazapropyl]-*n*-pentyl]-	5.55	1.16
15	1,3-oxazole-4-carboxylic acid, 4,5-dihydro-5-(1-methylethyl)-, ethyl ester	5.625	1.19
16	3-Amino-4,5-dimethyl-2(5H)-furanone	5.792	1.56
17	3-Methyl-4,6-dioxanonane	6.483	0.49
19	4,8,12-Trimethyltridecan-4-olide	6.925	1.02
20	7-Methoxy-2H-1,3-benzodioxol-5-amine	7	0.53
21	2-Amino-4-methyl-3-nitropyridine	7.208	0.77
22	Cyclopentanone, 2-(3-methyl-2-buten-1-yl)-	7.467	0.72
23	Tetradecane	7.675	2.32
24	Z-10-Tetradecen-1-ol acetate	7.867	1.00
25	3-Hepten-2-one, *O*-methyloxime	8.183	1.30
26	9-Methyl-Z-10-pentadecen-1-ol	8.3	2.84
30	9-Aza-1-methylbicyclo [3.3.1]nonan-3-ol	8.358	1.40
31	Benzoic acid, 2,5-dimethyl-	8.658	0.78
32	Benzaldehyde-2-acetyloxy-, aminocarbonyl hydrazone	8.875	0.82
33	*p*-Cymene-2,5-diol	9.667	0.73
34	Hexadecane	10.167	1.91
35	4H-1,4-Epoxy-4a,7-methanonaphthalene, 1,5,6,7,8,8a-hexahydro-,	11.258	1.27
36	1-Benzoxirene, 1a-[2-(2-methyl-1,3-dioxolan-2-yl)-1-ethenyl]perhydro-2,2,5a-trimethyl	11.342	2.38
37	3-*O*-Methyl-*d*-glucose	11.558	11.40
38	Adenine	12.417	0.61
39	2-Cyclohexen-1-one, 4-hydroxy-3,5,6-trimethyl-4-(3-oxo-1-butenyl)-	12.55	1.04
40	Allo-Inositol	13.325	0.82
41	Pyrrolo [1,2-a]pyrazine-1,4-dione, hexahydro-3-(2-methylpropyl)-	14.025	0.48
42	1-Naphthalenecarbonitrile, 8-amino-	14.608	0.71
43	Undecanoic acid	14.608	0.51
44	Phenol, 2-(1,1-dimethyl ethyl)-4-(1-methyl-1-phenylethyl)-	15.1	0.42
45	Phenol, 2,6-bis(1,1-dimethylethyl)-4-(1-methyl-1-phenylethyl)-	15.567	0.46
46	Hexadecanoic acid, 2-hydroxy-1-(hydroxymethyl)ethyl ester	19.317	0.42
47	Phenol, 2,4-bis(1-methyl-1-phenylethyl)-	19.517	1.28
48	2,4-Bis(dimethylbenzyl)-6-*t*-butylphenol	19.642	0.96
49	tert-Butylhydroquinone, diacetate	21.058	0.49
50	13-Docosenamide, (Z)-	21.461	1.94

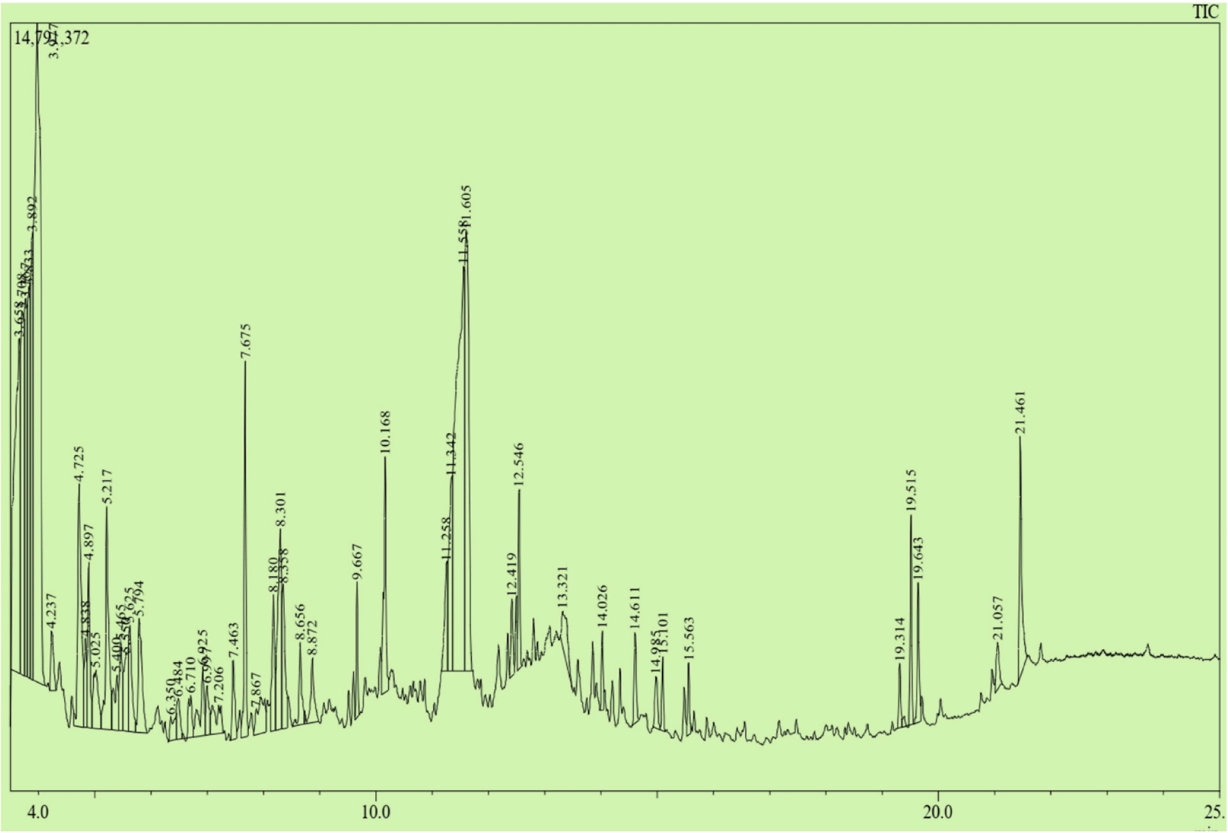

Fig. 1. The bioactive compounds extracted from the PH were analyzed by gas chromatography (GC-2010 plus, Shimadzu Corporation, Kyoto, Japan), coupled with a mass spectrometer (GCMS- TQ 8040, Shimadzu Corporation, Kyoto, Japan). A fused silica capillary column (Rxi-5ms; 30 m, 0.25 mm ID, and 0.25 μm) was used for GC maintaining sample inlet temperature at 250 °C. 1 μL sample was injected in *splitless* mode. The oven temperature was programmed as 75 °C (1 min); 25 °C, 125 °C (1min); 10 °C, 300 °C (15min). The aux (GC to MS interface) temperature was set to 250 °C. The total run time was 36.50 min and the column flow rate was 1.5 mL/min He gas.

μg/mL and 0.54 μg/mL (Fig. 2e and f).

3.3. *Weekly body weight and blood glucose levels of the animals*

The body weights of animals throughout the intervention are shown in Fig. 3a. It shows that after three weeks, the body weight of o NC group was higher than all other groups although the body weights of other groups except the DC group increased from their initial weights. In the case of the treatment group, it shows the body weight of the PHAgNP20 group was increased significantly ($P < 0.05$) in comparison to the DC group.

The fasting blood glucose levels throughout the intervention period are shown in Fig. 3b. After the end of 3rd week, the fasting blood glucose levels of all treatment groups such as PH200, PH100 & PHAgNP20 decreased compared with the DC group. The data for the OGTT test is shown in Fig. 3c. It showed the blood glucose levels of all treatment groups were increased significantly after 30 min and restored after 120 min.

3.4. *Effect of treatment on the relative pancreas, kidney, and liver weights and serum parameters*

The effects of PH on weight changes of organs and biochemical parameters are summarized in Table 4. Liver weights of the DC group were found to be lower than NC, PH200 & PH100, and RC groups. On the other hand, the pancreas weights of RC were significantly ($P < 0.05$) lower than other groups. Among the biochemical parameters, the serum ALT level of DC was higher than all other groups. The PHAgNP20 was found to normalize the ALT level significantly ($P < 0.01$) compared to the DC group. In the case of AST level, PH200 lowered the AST level significantly compared to the DC group. In the case of ALP level, the ALP level of PH200 is significant compared to the RC group and NC group. But PH100 and PHAgNP20 showed lower levels of ALP compared to the NC group. It showed that the level of total protein in the DC group was significantly higher than in all other groups. The total protein levels are equal both in NC and PHAgNP20 groups. The total protein level in PH200 & PH100 groups was lower than in the DC group.

Total cholesterol and triglyceride levels are shown in Fig. 4a. In the case of total cholesterol level, group PH200 was found to be

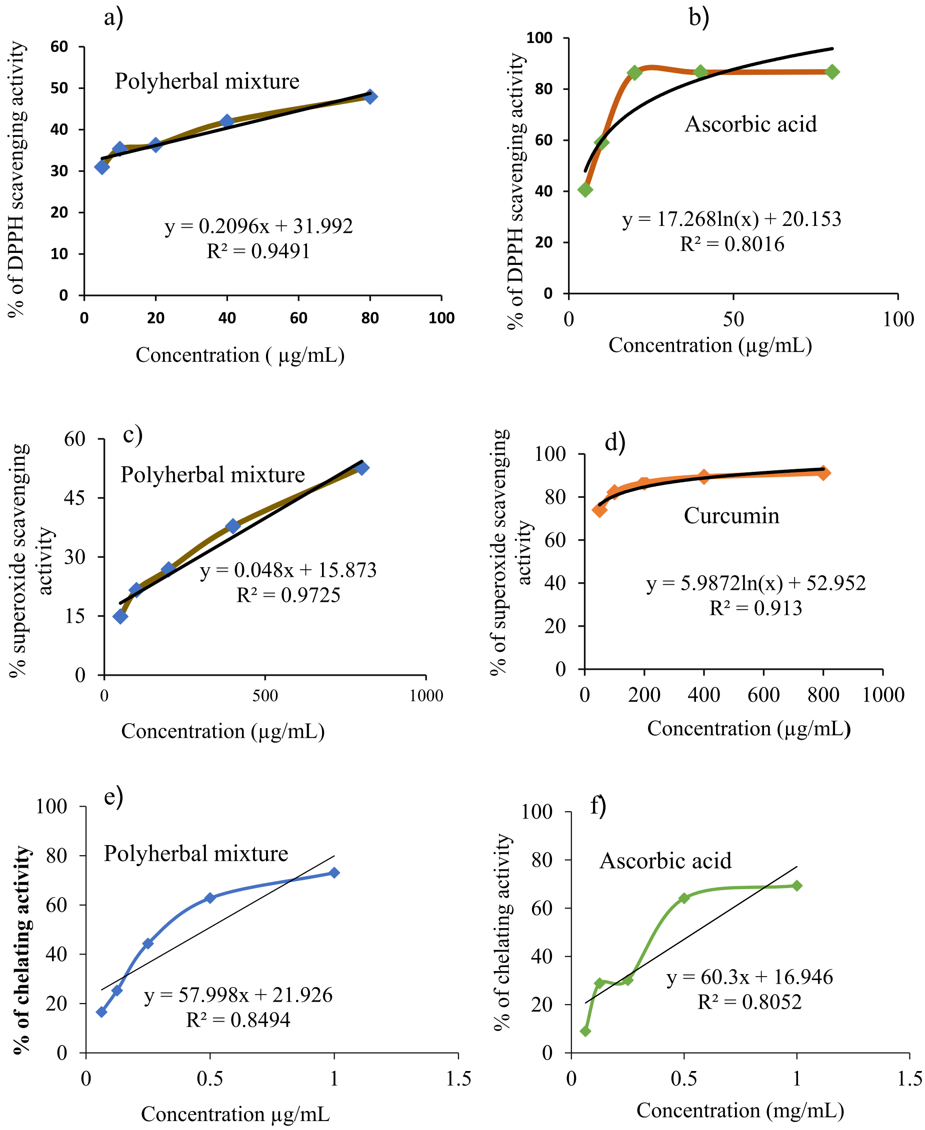

Fig. 2. DPPH scavenging activity of different concentrations of polyherbal extract and standard ascorbic acid (AA) and comparative IC50 values. Superoxide scavenging activity of different concentrations of polyherbal extract and standard curcumin and comparative IC50 values. The iron chelating activity of different concentrations of polyherbal extract and standard ascorbic acid and comparative IC50 values.

most effective in lowering the total cholesterol and triglycerides level and the values were significant ($P < 0.05$) compared to the DC group. Serum creatinine and uric acid levels are shown in Fig. 4b. Serum creatinine level was significantly higher in the DC group. All treatment groups were found to impact reducing the creatinine level, however; PH100 most significantly reduced the creatinine and serum urea level (Fig. 4c) in comparison to the DC group. The uric acid level of PH200 was close to the NC group.

3.5. Histopathological analysis of pancreas and kidney

The histological images and scoring for the changes in pancreatic tissue of experimental animal groups are shown in Fig. 5a and Table 5, respectively. In the DC group, pancreatic tissue was found to be more degenerated compared to the NC group. On the other hand, among the treatment groups, PH200 showed less degeneration compared to the DC group. The diameter of the islet of Langerhans cells ($162 \pm 2.05\ \mu m^2$) for the PHAgNP20 was found to be reversed to the normal control while no necrotic cells are observed in this group. The tissue architecture for the kidney and the scoring of the changes are presented in Fig. 5b and Table 6, respectively. In the DC group, kidney tissue was found to be more necrotic compared to the NC group. On the other hand, among the treatment group, PH200 showed less necrotic compared to the DC group. The epithelial tubular cell degeneration, secretion of eosinophils in the lumen, and epithelial tubular cell necrosis in the diabetic control group were highly observed and the PH200 was found to minimize the

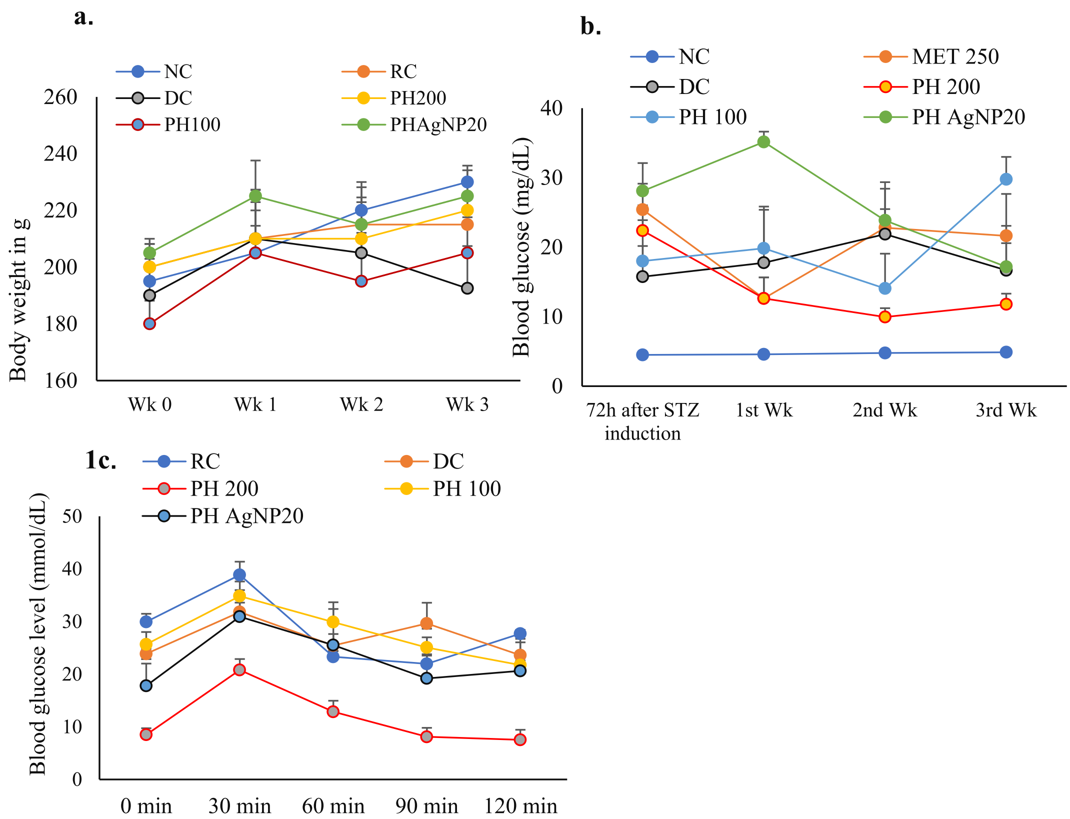

Fig. 3. Effect of polyherbal extract on **a.** Body weights; **b.** Weekly blood glucose levels; and **c.** Oral glucose tolerance test of different animal groups (n = 5). Data are shown as mean ± SME. Data were analyzed by One Way ANOVA followed by Dunnett's test (Graph Pad Prism 9.1.2) for multiple comparisons. RC, reference control (MET250); DC-Diabetic Control; PH200-Polyherbal Extract 200 mg/kg BW; PH100-Polyherbal extract 100 mg/kg BW; PHAgNP20-polyherbal extract silver nanoparticle 20 mg/kg BW; NC normal control.

Table 4
Effect of polyherbal extract on the weight of Pancreas, kidney, liver, biochemical enzymatic parameters in STZ induced albino rat (n = 3).

Parameter	NC	RC	DC	PH200	PH100	PHAgNP20
Relative pancreas Weight (g)	0.55 ± 0.07**	0.35 ± 0.02*	0.29 ± 0.03**	0.35 ± 0.02*	0.36 ± 0.02*	0.35 ± 0.04*
Relative kidney Weight (g)	1.86 ± 0.13	1.92 ± 0.03	1.60 ± 0.05	1.82 ± 0.04	1.85 ± 0.06	2.04 ± 0.07
Relative liver Weight (g)	8.31 ± 0.14	8.15 ± 0.94	7.79 ± 0.62	8.60 ± 0.86	7.83 ± 0.41	6.61 ± 0.14
AST (u/L)	5.20 ± 0.46	7.20 ± 0.3	7.80 ± 0.40***	2.53 ± 0.49***	2.82 ± 0.84**	6.67 ± 1.26
ALT (u/L)	70.67 ± 9.40*	87.33 ± 9.33	87.67 ± 2.96***	75.33 ± 6.57*	76.67 ± 4.91**	38 ± 4.73**
Alkaline phosphatase (u/L)	268.33 ± 15.10***	474.33 ± 50.60	632 ± 41.53***	723 ± 23.52	318.33 ± 67.66**	357.67 ± 67.34**
Total Protein (g/dL)	4.60 ± 0.67***	7.13 ± 0.53**	12.67 ± 1.20***	8.53 ± 1.03*	10.30 ± 1.06	7.27 ± 0.44**

Data are shown as Mean ± SME.

highest degeneration of kidney tissue.

4. Discussion

This study has synthesized silver nanoparticles of polyherbal extract using a green synthesis process which is an eco-friendly and economic approach to nanoparticle synthesis [31]. The remarkable physicochemical, and biological natures of silver nanoparticles enable them to act as useful nanoscale materials to be exploited across many therapeutic objectives [32]. The research focused on unfolding the effect of synthesized PHAgNP on reducing the necrosis of pancreatic beta cells. An attempt has also been made to establish how effective this nanoparticle is in streptozotocin-induced diabetes-related complications such as diabetic nephropathy using animal models. The green-synthesized silver nanoparticles (AgNPs), generally obtained by mixing plant extracts and silver salts (especially $AgNO_3$), are commonly used due to their high solubility, and slower release of silver ions during synthesis [33,34]. *In vivo* use of these nanoparticles in animal models is a common approach to evaluating the anti-diabetic effects while the polyherbal approach is also well documented in the ancient literature for their effective and extended therapeutic potential over single herbs [34].

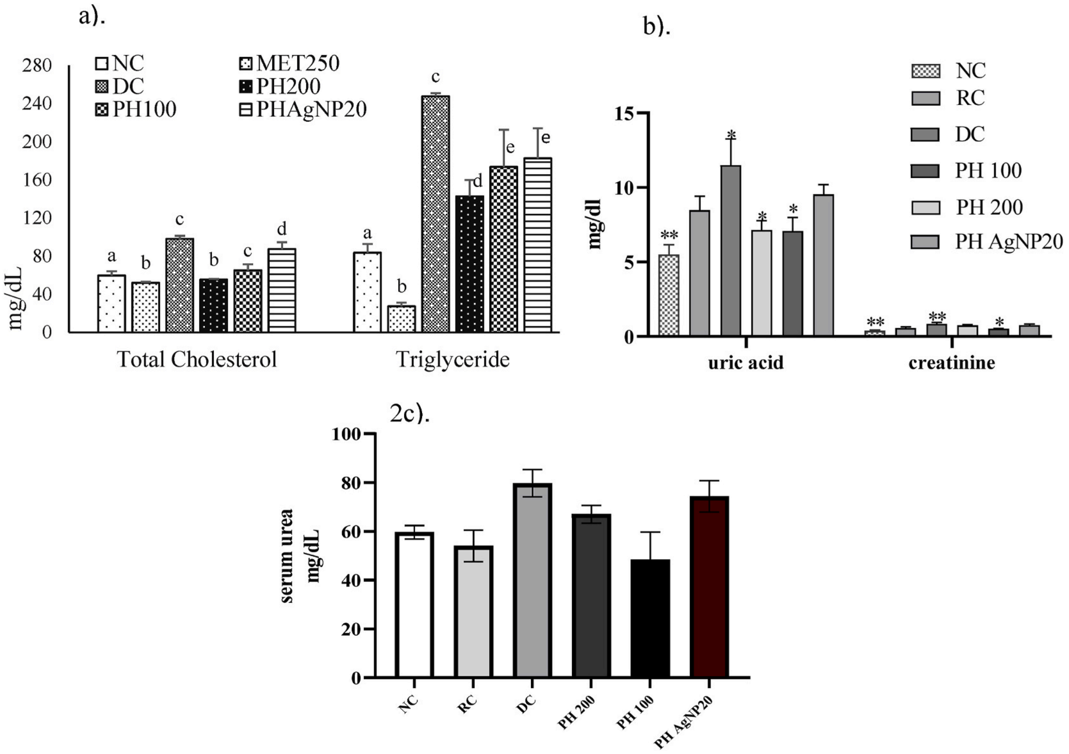

Fig. 4. Effect of polyherbal extract on **a)** Serum total cholesterol and triglyceride; **b)** Serum uric acid, creatinine, and **c)** serum urea levels of six animals. Data are shown as Mean ± SEM. Data were analyzed by One Way of Analysis of Variance (ANOVA) with Dunnett's test using GraphPad Prism 9.1.2. RC, reference control (MET250); DC-Diabetic Control; PH200-Polyherbal Extract 200 mg/kg BW; PH100-Polyherbal extract 100 mg/kg BW; PHAgNP20-polyherbal extract silver nanoparticle 20 mg/kg BW; NC normal control.

In recent times, many researchers have tried to explore the antidiabetic role of silver nanoparticles using the herbal formulations of *Glycosmis pentaphylla, Tridax procumbens, Mangifera indica, Bacopa monnieri, Hippophae rhamnoides, Dioscorea bulbifera, Eugenia jambolana, Gymnema sylvestre, Momordica charantia, Andrographis paniculate, and Myristica fragrans.* This research has postulated mixing the polyherbal component (5:2:2:1) based on their individual polyphenolic contents because the polyphenolic compounds are strongly associated with antidiabetic action, thus working as an analog or metabolic enzyme inhibitor or insulin stimulator to normalize pancreatic β-cells [35–37].

The initial phytochemical analysis and the gas chromatography-mass spectroscopy data showed that the polyherbal extract is abundant with plant phenolic, terpenoids, saponins, and steroids. Terpenoids and saponins are reported to show antidiabetic effects attenuating blood glucose by the inhibition of gluconeogenesis and glycogenolysis and insulin-like activity [38]. Saponins are likely to alleviate hyperglycemia-associated oxidative stress in type 2 diabetes while tannins extracted from different plant materials are noticed to inhibit α-amylase and α-glucosidase activities, thus decreasing glucose transport through the intestinal epithelium [39,40]. Some of the terpenoids, tannins, and saponins are highly effective to show antioxidative effects. Some of our GC-MS compounds such as 2-Furanone, 3,4-dihydroxy tetrahydro, are reported as insulin secretors while 3-*O*-Methyl-*d*-glucose, Phenol, 2,4-bis(1-methyl-1-phenylmethyl)- are cited as antihyperglycemic [41]. The antioxidative functions of our polyherbal extract are noticed with potential free radical scavenging effects measured in terms of inhibition concentrations of cut-off value less than 1000 μg/mL. These phytocomponent-based antioxidative effects might act individually or in combination to increase glycolytic enzyme activity, which could explain why polyherbal extracts are anti-diabetic [41].

The observed loss of an animal's body weight is a common phenomenon in STZ-induced hyperglycemia which is evident to be caused due to increased muscle wasting and protein loss in tissues. Diabetes is typically characterized by a drop in body weight and an increase in food and fluid intake due to the destruction of β-cells brought on by metabolic changes causing inadequate or unavailable insulin supply [42]. Plant extracts can substantially revert the situation through their biometabolites, and our results are consistent, especially for the dose of PHAgNP20. The synergistic effect of a polyherbal combination usually triggers better than single plants to maximize antidiabetic protection due to the nature of the compounds [43]. Additionally, nanoparticles enhance the action through their higher solubility and bioavailability achieved through the nanostructured particle size. The enriched polyphenolic status of our nano-based polyherbal extract might assist the effect. Blood glucose levels of treatment control groups were significantly reduced compared to the diabetic control group receiving no treatment. The ability of the PH to effectively increase body weight and reduce the blood glucose levels of diabetic rats may be attributed to its antihyperglycemic effect. Recent scientific findings attest to this result, with evidence of weight gain and increase oral glucose tolerance after treatment with polyherbal preparations [43]. The increase of

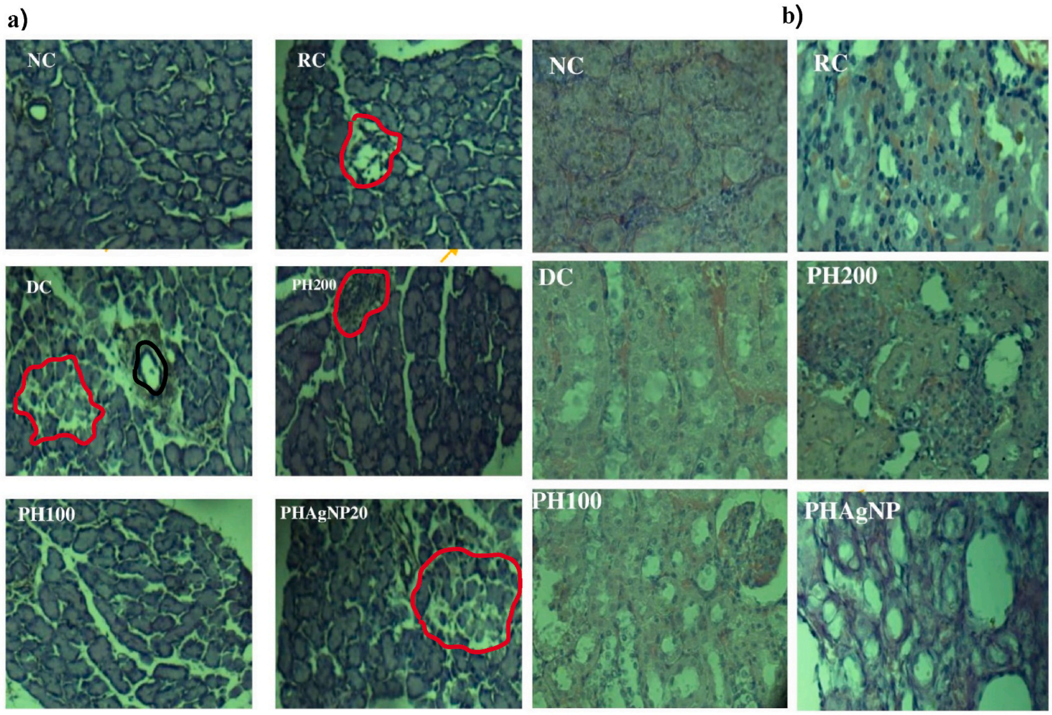

Fig. 5. Effect of polyherbal extract on the changes of tissue architectures of **a)** pancreatic islets and **b)** kidney tissues at the end of the intervention period examined at the magnification 10× 40. DC, diabetic control; RC, reference control (metformin 250 mg/kg BW); PH200, Polyherbal extract 200 mg/kg BW; PH100; Polyherbal extract 100 mg/kg BW; Polyherbal extract with silver nanoparticle 20 mg/kg BW; NC, normal control.

Table 5
Scoring for the effect of polyherbal extract on the pancreatic architectures.

Changes in Pancreatic Tissues						
	NC	RC	DC	PH200	PH100	PHAgNP20
Degenerated Cells	-	+	+	+	++	+
Diameter of islet of Langerhans (μm)	173 ± 47		125 ± 28	220 ± 18	205 ± 13	162 ± 2.05
The area occupied by β-cell/islet of ± Langerhans ($μm^2$)	20,703 ± 4730		11,227 ± 2309	46,400 ± 1861	30,450 ± 1366	43,700 ± 5773
Necrotic cells	-	+	++	+	+	+
Degenerated Cells	-	+	+	+	+	+

Scoring for the histopathological assessments of pancreatic tissues are graded as follows.
(−) indicates "No abnormality" (+) indicates "Mild injury"(++) indicates "Moderate injury"(++ +) indicates "Severe injury".

Table 6
Scoring for the effect of the polyherbal extract on the kidney architectures.

Changes in Kidney Tissues						
	NC	RC	DC	PH200	PH100	PHAgNP20
Epithelial tubular cell degeneration	–	+	–	–	++	–
Epithelial tubular cell necrosis	–	+	–	+	+	–
Increase of fibrous tissue	–	+	–	+	+	+
Interstitial hyperemic vessels	–	+	–	+	+	–
Secretion of eosinophils in the lumen	–	+	–	–	–	–
Glomerulus and tubular atrophic	–	++	–	+	+	+

Scoring for the histopathological assessments of kidney tissues are graded as follows.
(−) indicates "No abnormality" (+) indicates "Mild injury"(++) indicates "Moderate injury"(++ +) indicates "Severe injury".

oral glucose tolerance in the treatment group especially by the PHAgNP32 supports the antihyperglycemic action of the polyherbal extract.

The relative weight loss, of the kidneys and pancreas in diabetic control animals, is not inevitably and solely impacted by the hyperglycemic trend of the animals. However, relative kidney weight loss is associated with glomerular pathology and renal hypertrophy progression [44]. The histopathological scoring of the kidney supports the ameliorative effects in terms of the alleviation of epithelial tubular cell necrosis as well as interstitial hyperemic vessels. The decrease in the weight of the pancreas could be attributed to the disruption and disappearance of pancreatic islets and the selective destruction of insulin-producing cells reflected in our DC group. Additionally, the liver of treated animals compared to normal control was truncated which could be linked with the decreased triglyceride accumulation as shown by the treatment especially PHAgNP20 [45].

The liver is the prime organ for maintaining glucose homeostasis by controlling glycogenesis, glycolysis, glycogenolysis, and gluconeogenesis [46]. Therefore, liver function test in diabetes is a pivotal factor to evaluate the effect of therapeutic potentiality. In our study, liver function improvement is thought to be attested by the restoration of a specific liver marker serum alanine aminotransferase (ALT) by the treatment with PHAgNP20. The aspartate aminotransferase (AST) and alkaline phosphatases (ALP) are also significantly reverted to the normal state by PH100 and PHAgNP20. The AST is a cytoplasmic enzyme that releases into circulation due to the loss of structural integrity of the liver by STZ [46]. A significant decrease in AST could be ascribed as a complete or partial recovery of the damaged liver, which has been demonstrated in previous studies that antioxidant-rich plants can revert to the damaged liver by reducing oxidative stress [47]. The remarkable antioxidative status of PH is consistent with the previous observations. Total proteins are found to be elevated significantly compared to controls. The increase in total proteins may be accredited to the increase of acute phase proteins, fibrinogen, and globulins, together with a decrease in the synthetic rate of albumin due to insulin resistance/deficiency. However, the elevated total proteins were attenuated by PHAgNP20 implying its antidiabetic potential to protect pancreatic cells [48]. Total cholesterol, triglyceride, serum creatinine, urea, and uric acids were invariably minimized with the PH treatment. The polyherbal extract's ability to lower blood lipids may be a result of its ability to reduce hepatic cholesterol biosynthesis, enhance fecal bile acid secretion, stimulate receptor-mediated LDL-cholesterol catabolism, and improve liver uptake of LDL from blood [49]. An elevated level of serum urea and creatinine is a key indicator of renal impairment. In our study, diabetic groups had significantly higher serum levels of uric acid and creatinine than non-diabetics, and these levels were significantly reversed in the animals treated with polyherbal extracts, especially the HPAgNP20, demonstrating the renoprotective efficacy of the polyherbal extract [50]. The potential of the biosynthesized silver nanoparticle could be ascribed by their enhanced permeability to the cellular systems which are usually selective to the size of the plant-based molecules. Previous studies also reported the antidiabetic capacity of both silver nanoparticles as well as some other bioengineered nanoparticles that are more biocompatible, and accessible [51].

Histopathological analysis usually reflects the architectural changes of different tissues. The scoring of the pancreas and the kidney tissues in our experiments depicts the changes comprehensively. The pancreatic tissue sectioning showed severe cell degeneration in the diabetic control group whereas the normal control group, having a larger area occupied by the β cells, showed a more integrated

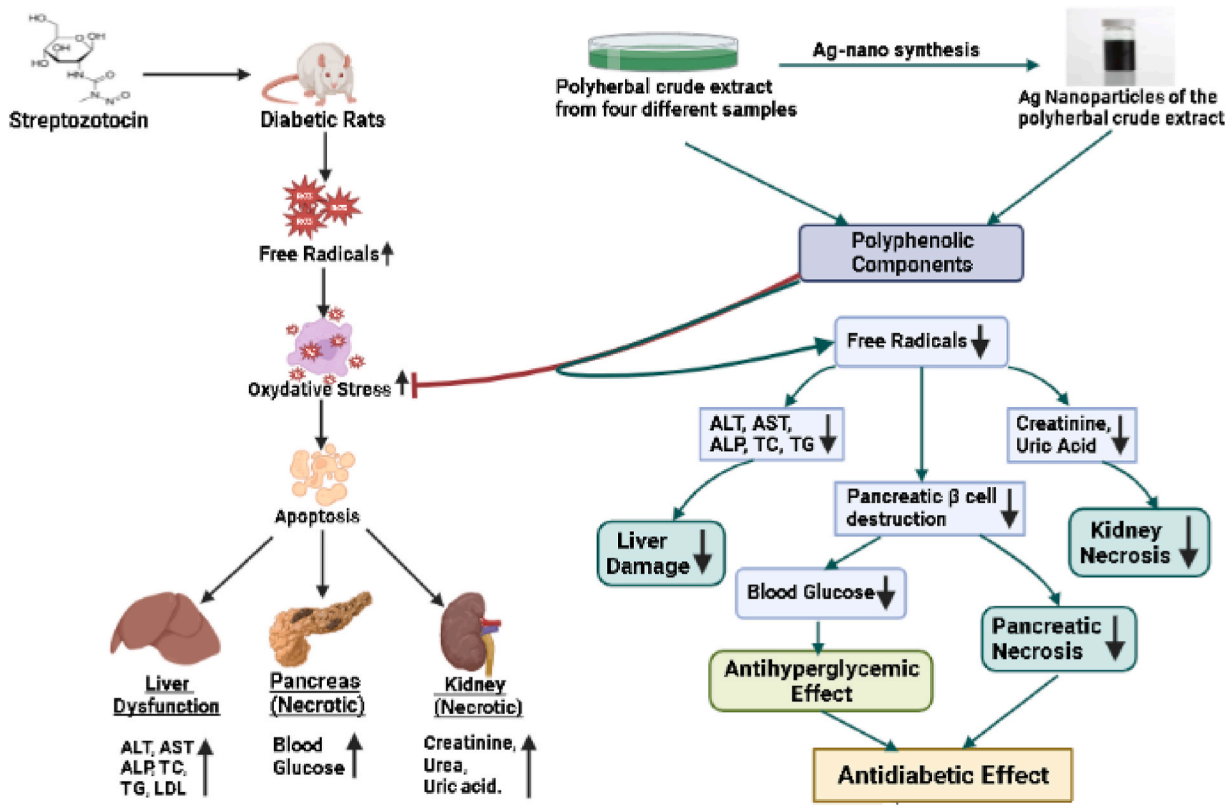

Fig. 6. Proposed mechanism for how the polyherbal extract can attenuate pancreatic dysfunction as well as diabetic complications.

structure although all other treatment groups had degeneration. Among the treatment groups, PH200 showed less degeneration and necrosis of pancreatic tissue which could be due to its higher bioavailability emphasizing to exert of the extensive regenerative potential of PH200. Diabetic kidney disease (DKD) is one of the most important long-term complications of diabetes and is among the leading causes of end-stage kidney disease (ESRD) in developed countries. It develops in approximately 10%–30% of patients with diabetes mellitus [52] and the overlap of diabetes mellitus and renal injury exponentially amplifies the risk of other diabetic secondary complications such as cardiovascular events and death. Therefore, a study on concomitant the effect of the therapeutic target in diabetes and diabetes-related parameters is inevitably important [53]. In our study, the histological examination of kidney tissue of the diabetic control group showed severe degeneration while no abnormality was observed in the normal control group. In terms of the scoring for epithelial tubular cell degeneration, epithelial tubular cell necrosis, and secretion of eosinophils in the lumen, the diabetic control group was shown to be highly inflamed. And the PH200 was displayed to minimize the highest tissue degeneration implying that the tubular necrosis and tubular degeneration caused by STZ-induction could be improved at least in the experimental condition through the treatment with the polyherbal extract. This could be possibly underlined by the recovery from the direct damage to the kidney tissues which is generally believed to be mediated by Glut 2 uptake in proximal tubule cells, causing acute tubular necrosis and subsequent changes in tubular cell degeneration, tubular cell necrosis, and other kidney function markers [54].

Additionally, the antioxidative potential of polyherbal extract might have a significant contribution to such improvement as the researchers postulated a strong correlation between the antioxidative capacity and healing of STZ-induced necrotic tissues (a proposed mechanism is shown in Fig. 6) [55]. Additionally, the antioxidant molecules build the cellular defense by upregulating the antioxidative enzymes leading to attenuating the oxidative stress to normalize the serum biochemical markers and tissue architecture. The greater bioavailability of the plant extract-based nanoparticles may foster the process of cellular defense [56] as evident for silver nanoparticles which function as a potential antioxidant [57].

5. Conclusion

This research prepared the silver nanoparticles using polyherbal extract and evaluated the antioxidative and antidiabetic effects of resulting nanoparticles, especially focusing on the impact on pancreatic health. The polyherbal-based treatment showed strong antioxidative capacity and fully or partially normalized the serum liver enzymes, lipid profiles, and kidney parameters. Nanoformulation (PHAgNP20) of the polyherbal product exerted an added advantage in potentiating the antidiabetic effect by attenuating the necrosis of pancreatic tissues. The strong antioxidative effects of the PH have inculcated and corroborated the effects. However, the use of a single dose of PHAgNP20 impedes the impact of the study because multiple doses are preferred for drug discovery episodes. Therefore, a mechanism-based dose-response further study, as well as several layers of experimentation, on the extract are necessary before making the clinical conclusions to affirm the best use of the nanoparticle of polyherbal extract as therapeutic in diabetes mellitus.

Author contribution statement

Muhammad Abid Hasan Chowdhury: Performed the experiments; Wrote the paper.

Md Atiar Rahman: Conceived and designed the experiments; Analyzed and interpreted the data.

Salahuddin Quader Al Araby: Analyzed and interpreted the data, Performed the experiments; Wrote the paper.

Walla Alelwani, Shahad W. Kattan, Omniah A Mansouri, Jitbanjong Tangpong: Contributed reagents, materials, analysis tools or data; Analyzed and interpreted the data.

Mala Khan: Contributed reagents, materials, analysis tools or data.

Data availability statement

Data will be made available on request.

Funding

The research was supported by Walailak University, Thailand.

Declaration of competing interest

The authors declare that they have no known competing financial interests or personal relationships that could have appeared to influence the work reported in this paper.

Acknowledgment

The authors wish to thank the Research and Publication Cell, at the University of Chittagong for partially funding the research. We would like to thank the DNA and Hormone Laboratory for sponsoring the analysis of serum parameters. The authors would also like to thank DR. Zillur Rahman MBBS, M Phil (Pathology), Ph.D., former Associate Professor, Department of Pathology, Chittagong Medical College (Currently Professor at Bangabandhu Sheikh Mujib Medical University) to support in histopathological analysis and scoring.

The authors extend their thanks to the R & D of University of Jeddah, Saudi Arabia to support this research.

Appendix A. Supplementary data

Supplementary data to this article can be found online at https://doi.org/10.1016/j.heliyon.2023.e16137.

References

[1] M. Roden, G.I. Shulman, The integrative biology of type 2 diabetes, Nature 576 (2019) 51–60, https://doi.org/10.1038/s41586-019-1797-8.
[2] IDF Diabetes Atlas 2021, tenth ed., Access date: 19 January 2023.
[3] S. Dewanjee, S. Das, A.K. Das, N. Bhattacharjee, A. Dihingia, T.K. Dua, J. Kalita, P. Manna, Molecular mechanism of diabetic neuropathy and its pharmacotherapeutic targets, Eur. J. Pharmacol. 833 (2018) 472–523, https://doi.org/10.1016/j.ejphar.2018.06.034.
[4] S. Dewanjee, N. Bhattacharjee, MicroRNA: a new generation therapeutic target in diabetic nephropathy, Biochem. Pharmacol. 155 (2018) 32–47, https://doi.org/10.1016/j.bcp.2018.06.017.
[5] N. Aryaeian, S.K. Sedehi, T. Arablou, Polyphenols and their effects on diabetes management: a review, Med. J. Islam. Repub. Iran 31 (2017) 134, https://doi.org/10.14196/mjiri.31.134.
[6] P. Sudha, S.S. Zinjarde, S.Y. Bhargava, A.R. Kumar, Potent α-amylase inhibitory activity of Indian Ayurvedic medicinal plants, BMC Compl. Alternative Med. 11 (2011) 5, https://doi.org/10.1186/1472-6882-11-5.
[7] S.A.A. Rizvi, A.M. Saleh, Applications of nanoparticle systems in drug delivery technology, Saudi Pharmaceut. J. 26 (2018) 64–70, https://doi.org/10.1016/j.jsps.2017.10.012.
[8] N. SreeHarsha, A. Shariff, Y.A. Shendkar, B.E. Al-Dhubiab, G. Meravanige, Development and evaluation of a (SEDDS) self—emulsifying drug delivery system for darifenacin hydrobromide, Indian J. Pharm. Educ. Res. 53 (2019) 204–212.
[9] S. Faisal, S.A. Shah, S. Shah, M.T. Akbar, F. Jan, I. Haq, M.E. Baber, K. Aman, F. Zahir, F. Bibi, F. Syed, M. Iqbal, S.M. Jawad, S. Salman, In vitro biomedical and photo-catalytic application of bio-inspired *Zingiber officinale* mediated silver nanoparticles, J. Biomed. Nanotechnol. 16 (4) (2020) 492–504, https://doi.org/10.1166/jbn.2020.2918.
[10] N. Krithiga, A. Rajalakshmi, A. Jayachitra, Green synthesis of silver nanoparticles using leaf extracts of clitoria ternatea and Solanum nigrum and study of its antibacterial effect against common nosocomial pathogens, J. Nanoscience. 2015 (2015) 1–8, https://doi.org/10.1155/2015/928204.
[11] S. Pachava, S. Puttachari, A. Shariff, R.S. Thakur, Formulation and evaluation of solid self microemulsifying drug delivery system of a selective second generation cephalosporin antibiotic, Int. J. Pharmaceut. Sci. Rev. Res. 24 (2014) 176–181.
[12] S. Jadoun, R. Arif, N.K. Jangid, R.K. Meena, Green synthesis of nanoparticles using plant extracts: a review, Environ. Chem. Lett. 19 (2021) 355–374, https://doi.org/10.1007/s10311-020-01074-x.
[13] M.F. Mahmoud, F.E.Z.Z. el Ashry, N.N. el Maraghy, A. Fahmy, Studies on the antidiabetic activities of *Momordica charantia* fruit juice in streptozotocin-induced diabetic rats, Pharm. Biol. 55 (2017) 758–765, https://doi.org/10.1080/13880209.2016.1275026.
[14] S. Pelegrin, F. Galtier, A. Chalançon, J.P. Gagnol, A.M. Barbanel, Y. Pélissier, et al., Effects of *Nigella sativa* seeds (black cumin) on insulin secretion and lipid profile: a pilot study in healthy volunteers, Br. J. Clin. Pharmacol. 85 (2019) 1607–1611, https://doi.org/10.1111/bcp.13922.
[15] A.E. Koshak, N.M. Yousif, B.L. Fiebich, E.A. Koshak, M. Heinrich, Comparative immunomodulatory activity of *Nigella sativa* L. preparations on proinflammatory mediators: a focus on asthma, Front. Pharmacol. 9 (2018) 1075, https://doi.org/10.3389/fphar.2018.01075.
[16] H.S. Mahmoud, A.A. Almallah, H.N. Gad El-Hak, T.S. Aldayel, H.M.A. Abdelrazek, H.E. Khaled, The effect of dietary supplementation with *Nigella sativa* (black seeds) mediates immunological function in male Wistar rats, Sci. Rep. 11 (1) (2021) 7542, https://doi.org/10.1038/s41598-021-86721-1.
[17] G.A. Geberemeskel, Y.G. Debebe, N.A. Nguse, Antidiabetic effect of fenugreek seed powder solution (*Trigonella foenum-graecum* L.) on hyperlipidemia in diabetic patients, J. Diabetes Res. (2019), 8507453, https://doi.org/10.1155/2019/8507453.
[18] M. Baset, T. Ali, H. Elshamy, A. el Sadek, D. Sami, M. Badawy, et al., Anti-diabetic effects of fenugreek (*Trigonella foenum-graecum*): a comparison between oral and intraperitoneal administration—an animal study, Int. J. Funct. Nutr. 1 (1) (2020) 2, https://doi.org/10.3892/ijfn.2020.2.
[19] R.A. Antora, R.M. Salleh, Antihyperglycemic effect of Ocimum plants: a short review, Asian Pac. J. Trop. Biomed. 7 (2017) 755–759, https://doi.org/10.1016/j.apjtb.2017.07.010.
[20] S. Parasuraman, S. Balamurugan, P.V. Christapher, R.R. Petchi, W.Y. Yeng, J. Sujithra, et al., Evaluation of antidiabetic and antihyperlipidemic effects of hydroalcoholic extract of leaves of *Ocimum tenuiflorum* (Lamiaceae) and prediction of biological activity of its phytoconstituents, Pharmacogn. Res. 7 (2015) 156–165, https://doi.org/10.4103/0974-8490.151457.
[21] M.A. Aziz, Qualitative phytochemical screening and evaluation of anti-inflammatory, analgesic and antipyretic activities of *Microcos paniculata* barks and fruits, J. Integr. Med. 13 (2015) 173–184, https://doi.org/10.1016/S2095-4964(15)60179-0.
[22] G. Singh, A.K. Passsari, V.V. Leo, V.K. Mishra, S. Subbarayan, B.P. Singh, B. Kumar, S. Kumar, V.K. Gupta, H. Lalhlenmawia, S.K. Nachimuthu, Evaluation of phenolic content variability along with antioxidant, antimicrobial, and cytotoxic potential of selected traditional medicinal plants from India, Front. Plant Sci. 7 (2016) 407, https://doi.org/10.3389/fpls.2016.00407.
[23] E.A. Ainsworth, K.M. Gillespie, Estimation of total phenolic content and other oxidation substrates in plant tissues using Folin-Ciocalteu reagent, Nat. Protoc. 2 (2007) 875–877, https://doi.org/10.1038/nprot.2007.102.
[24] S.D. Sanja, N.R. Sheth, N.K. Patel, D. Patel, B. Patel, Characterization and evaluation of the antioxidant activity of *Portulaca oleracea*, Int. J. Pharm. Pharmaceut. Sci. 1 (2009) 74–84.
[25] M.M. Pandey, R. Govindarajan, A.K.S. Rawat, P. Pushpangadan, Free radical scavenging potential of Saussarea costus, Acta Pharm. 55 (2005) 297–304.
[26] I.F.F. Benzie, J.J. Strain, The ferric reducing ability of plasma (FRAP) as a measure of "'Antioxidant power': the FRAP assay, Anal. Biochem. 239 (1) (1996) 70–76.
[27] J. Suresh, R. Yuvakkumar, M. Sundrarajan, S.I. Hong, Green synthesis of magnesium oxide nanoparticles, Adv. Mater. Res. 952 (2014) 141–144. https://dx.doi.org/10.4028/www.scientific.net/AMR.952.141.
[28] K. Govindaraju, K.V. Anand, S. Anbarasu, J. Theerthagiri, S. Revathy, P. Krupakar, et al., Seaweed (*Turbinaria ornata*)-assisted green synthesis of magnesium hydroxide [Mg(OH)2] nanomaterials and their anti-mycobacterial activity, Mater. Chem. Phys. 239 (1) (2020), 122007, https://doi.org/10.1016/j.matchemphys.2019.122007.
[29] R.D. Wilson, M.S. Islam, Fructose-fed streptozotocin-injected rat: an alternative model for type 2 diabetes, Pharmacol. Rep. 64 (2012) 129–139, https://doi.org/10.1016/S1734-1140(12)70739-9.
[30] S.Q. Al-Araby, M.A. Rahman, M.A.H. Chowdhury, R.R. Das, T.A. Chowdhury, C.M.M. Hasan, M. Afroze, M.A. Hashem, D. Hajjar, W. Alelwani, A.A. Makki, M. A. Haque, *Padina tenuis* (marine alga) attenuates oxidative stress and streptozotocin-induced type 2 diabetic indices in Wistar albino rats, South Afr. J. Bot. 128 (2020) 87–100, https://doi.org/10.1016/j.sajb.2019.09.007.
[31] N.S. Abdullah, Al-Radadi, T. Hussain, S. Faisal, S.A.R. Shah, Novel biosynthesis, characterization and bio-catalytic potential of green algae (*Spirogyra hyalina*) mediated silver nanomaterials, Saudi J. Biol. Sci. 29 (2022) 411–419, https://doi.org/10.1016/j.sjbs.2021.09.013.

[32] S. Faisal, M.A. Khan, H. Jan, S.A. Shah, Abdullah, S. Shah, M. Rizwan, M.T. Akbar Wajidullah, Redaina, Edible mushroom (*Flammulina velutipes*) as biosource for silver nanoparticles: from synthesis to diverse biomedical and environmental applications, Nanotechnology 32 (2020), 065101, https://doi.org/10.1088/1361-6528/abc2eb.
[33] E.K. Kambale, C.I. Nkanga, B.P.I. Mutonkole, A.M. Bapolisi, D.O. Tassa, J.M.I. Liesse, R.W.M. Krause, P.B. Memvanga, Green synthesis of antimicrobial silver nanoparticles using aqueous leaf extracts from three Congolese plant species (*brillantaisia patula, crossopteryx febrifuga* and *Senna siamea*), Heliyon 6 (2020), e04493.
[34] P. Anbazhagan, K. Murugan, A. Jaganathan, V. Sujitha, C.M. Samidoss, S. Jayashanthani, P. Amuthavalli, A. Higuchi, S. Kumar, H. Wei, et al., Mosquitocidal, antimalarial and antidiabetic potential of *musa paradisiaca*-synthesized silver nanoparticles: in vivo and in vitro approaches, J. Cluster Sci. 28 (2017) 91–107.
[35] R. Petchi, C. Vijaya, S. Parasuraman, Antidiabetic activity of polyherbal formulation in streptozotocin- Nicotinamide induced diabetic Wistar rats, J Tradit Complement Med 4 (2014) 108–117, https://doi.org/10.4103/2225-4110.126174.
[36] P. Upadhyay, Effect of a novel polyherbal formulation on diabetes induced memory deficits in rats, Clin. Exp. Pharmacol. 5 (2015) 6, https://doi.org/10.4172/2161-1459.1000194.
[37] T. Nagja, K. Vimal, A. Sanjeev, Anti-diabetic activity of a polyherbal formulation in streptozotocin-induced type 2 diabetic rats, J. Nat. Remedies 16 (2016) 148–152, https://doi.org/10.18311/jnr/2016/15323.
[38] S. Singh, M. Farswan, S. Ali, M. Afzal, F.A. Al-Abbasi, I. Kazmi, F. Anwar, Antidiabetic potential of triterpenoid saponin isolated from *Primula denticulate*, Pharm. Biol. 52 (6) (2014) 750–755, https://doi.org/10.3109/13880209.2013.869759.
[39] M.O. Nafiu, A.O.T. Ashafa, Antioxidant and inhibitory effects of saponin extracts from *Dianthus basuticus* burtt davy on key enzymes implicated in type 2 diabetes *In vitro*, Phcog. Mag. 13 (52) (2017) 576–582, https://doi.org/10.4103/pm.pm_583_16.
[40] Z.D. Kifle, S.G. Debeb, Y.M. Belayneh, *In vitro* α-amylase and α-glucosidase inhibitory and antioxidant activities of the crude extract and solvent fractions of *Hagenia abyssinica* leaves, BioMed Res. Int. 2021 (2021), 6652777, https://doi.org/10.1155/2021/6652777.
[41] N. Tran, B. Pham, L. Le, Bioactive compounds in anti-diabetic plants: from herbal medicine to modern drug discovery, Biology 9 (9) (2020) 252, https://doi.org/10.3390/biology9090252.
[42] M.I.M. Khalil, M.M. Ibrahim, G.A. El-Gaaly, A.S. Sultan, *Trigonella foenum* (Fenugreek) induced apoptosis in hepatocellular carcinoma cell line, HepG2, mediated by upregulation of p53 and proliferating cell nuclear antigen, BioMed Res. Int. (2015), 914645, https://doi.org/10.1155/2015/914645.
[43] S. Srivastava, V.K. Lal, K.K. Pant, Polyherbal formulations based on Indian medicinal plants as antidiabetic phytotherapeutics, Phytopharmacology 2 (2012) 1–15.
[44] N. Tsuboi, Y. Okabayashi, A. Shimizu, T. Yokoo, The renal pathology of obesity, Kidney Int Rep 2 (2) (2017) 251–260, https://doi.org/10.1016/j.ekir.2017.01.007.
[45] H. Merzouk, S. Madani, D.C. Sari, J. ProstM. Bouchenak, J. Belleville, Time course of changes in serum glucose, insulin, lipids and tissue lipase activities in macrosomic offspring of rats with streptozotocin-induced diabetes, Clin. Sci. 98 (1) (2000) 21–30, https://doi.org/10.1042/cs0980021.
[46] H.S. Han, G. Kang, J.S. Kim, B.H. Choi, S.H. Koo, Regulation of glucose metabolism from a liver-centric perspective, Exp. Mol. Med. 48 (3) (2016) e218, https://doi.org/10.1038/emm.2015.122.
[47] S. Akhter, M.A. Rahman, J. Aklima, M.R. Hasan, J.M.K.H. Chowdhury, Antioxidative role of hatikana (*Leea macrophylla* roxb.) partially improves the hepatic damage induced by CCl_4 in wistar albino rats, BioMed Res. Int. (2015), 356729, https://doi.org/10.1155/2015/356729.
[48] T.Semra, Ç. Sait, K. Serhat, T. İsmail, Y. Ökkeş, The effect of *Pistacia terebinthus* extract on lipid peroxidation, glutathione, protein, and some enzyme activities in tissues of rats undergoing oxidative stress, Turk. J. Zool. 41(1) 9. https://doi.org/10.3906/zoo-1508-41.
[49] M. Ramchoun, T. Khouya, H. Harnafi, S. Amrani, C. Alem, M. Benlyas, C.F. Kasbi, E.H. Nazih, P. Nguyen, K. Ouguerram, Effect of aqueous extract and polyphenol fraction derived from *Thymus atlanticus* leaves on acute hyperlipidemia in the Syrian golden hamsters, evid based complement altern, Méd. 2020 (2020), 3282596, https://doi.org/10.1155/2020/3282596.
[50] E.C. Ogbodo, B.C. Ibeme, I.P. Ezeugwunne, A.N. Okpogba, R.A. Analike, V.N. Oguaka, A.K. Amah, Effect of *phyllantus amarus* leaf extract on the serum creatinine, urea, and uric acid levels of alloxan-induced diabetic albino wistar rats, Int. J. Trend. Res. Dev. 5 (2018) 237–240.
[51] S. Faisal, H. Jan, Abdullah, I. Alam, M. Rizwan, Z. Hussain, K. Sultana, Z. Ali, M.N. Uddin, *In vivo* analgesic, anti-inflammatory, and anti-diabetic screening of *Bacopa monnieri*-synthesized copper oxide nanoparticles, ACS Omega 7 (2022) 4071–4082.
[52] G. Danaei, M.M. Finucane, Y. Lu, G.M. Singh, M.J. Cowan, C.J. Paciorek, J.K. Lin, F. Farzadfar, Y.H. Khang, G.A. Stevens, et al., National, regional, and global trends in fasting plasma glucose and diabetes prevalence since 1980: systematic analysis of health examination surveys and epidemiological studies with 370 country-years and 2.7 million participants, Lancet 378 (2011) 31–40.
[53] S.M. Doshi, A.N. Friedman, Diagnosis and management of type 2 diabetic kidney disease, Clin. J. Am. Soc. Nephrol. 12 (2017) 1366–1373.
[54] Y.-C. Tay, Y. Wang, L. Kairaitis, G.K. Rangan, C. Zhang, D.C.H. Harris, Can murine diabetic nephropathy be separated from superimposed acute renal failure? Kidney Int. 68 (2005) 391–398.
[55] F. Sharmen, M.A. Rahman, A.M.A. Ahmed, T.A. Siddique, M.K.J. Rafi, J. Tangpong, Upregulation of antioxidative gene expression by *Lasia spinosa* organic extract improves the predisposing biomarkers and tissue architectures in streptozotocin-induced diabetic models of long evans rats, Antioxidants 11 (12) (2020) 2398, https://doi.org/10.3390/antiox11122398.
[56] M. Sharma, A. Afaque, S. Dwivedi, Z.S. Jairajpuri, Y. Shamsi, M.F. Khan, M.I. Khan, D. Ahmed, *Cichorium intybus* attenuates streptozotocin-induced diabetic cardiomyopathy via inhibition of oxidative stress and inflammatory response in rats, Interdiscipl. Toxicol. 12 (3) (2019) 111–119, https://doi.org/10.2478/intox-2019-0013.
[57] A.K. Mittal, A. Kaler, U.C. Banerjee, Free radical scavenging and antioxidant activity of silver nanoparticles synthesized from flower extract of Rhododendron dauricum, NANO Biomed. Eng. 4 (3) (2012) 118–124.